# Robust method to retrieve the constitutive effective parameters of metamaterials

Xudong Chen, Tomasz M. Grzegorczyk, Bae-Ian Wu, Joe Pacheco, Jr., and Jin Au Kong
*Research Laboratory of Electronics, Massachusetts Institute of Technology, Cambridge, Massachusetts 02139, USA*
(Received 25 February 2004; published 26 July 2004)

We propose an improved method to retrieve the effective constitutive parameters (permittivity and permeability) of a slab of metamaterial from the measurement of *S* parameters. Improvements over existing methods include the determination of the first boundary and the thickness of the effective slab, the selection of the correct sign of effective impedance, and a mathematical method to choose the correct branch of the real part of the refractive index. The sensitivity of the effective constitutive parameters to the accuracy of the *S* parameters is also discussed. The method has been applied to various metamaterials and the successful retrieval results prove its effectiveness and robustness.

DOI: 10.1103/PhysRevE.70.016608 PACS number(s): 41.20.Jb, 42.25.Bs, 78.20.Ci

## I. INTRODUCTION

Left-handed (LH) structures have been realized so far as metamaterials [1–3] and very quickly, researchers have been working on retrieving their effective permittivity and permeability to better characterize them [4–6]. Known methods to date [7,8] use *S* parameters calculated from a wave incident normally on a slab of metamaterial, from which the effective refractive index $n$ and impedance $z$ are first obtained. The permittivity $\epsilon$ and permeability $\mu$ are then directly calculated from $\mu = nz$ and $\epsilon = n/z$.

It is also known that this retrieval process may fail in some instances, such as when the thickness of the effective slab (exhibiting bulk properties) is not accurately estimated [4] or when reflection ($S_{11}$) and transmission ($S_{21}$) data are very small in magnitude [6]. Although these issues have been addressed to some extent in previous works, we have found that the retrieved results in some cases are still unsatisfactory. In particular, the determination of the first boundary of the effective homogeneous slab, the selection of the sign of the roots when solving for the impedance $z$, the determination of the branch of the real part of refractive index $n$, and the origin of the spikes appearing in the retrieved impedance $z$, are many problems that deserve further investigation. The aforementioned issues are addressed in the next sections of this paper and some typical retrieval results are presented to show the robustness and effectiveness of the method. Note that the values of $\epsilon$, $\mu$, and $z$ are relative to those in free space, thus dimensionless.

## II. RETRIEVAL METHOD

### A. Theoretical retrieval equations

In order to retrieve the effective permittivity and permeability of a slab of metamaterial, we need to characterize it as an effective homogeneous slab. In this case, we can retrieve the permittivity and permeability from the reflection ($S_{11}$) and transmission ($S_{21}$) data. For a plane wave incident normally on a homogeneous slab of thickness $d$ with the origin coinciding with the first face of the slab, $S_{11}$ is equal to the reflection coefficient, and $S_{21}$ is related to the transmission coefficient $T$ by $S_{21} = Te^{ik_0 d}$, where $k_0$ denotes the wave number of the incident wave in free space. The *S* parameters are related to refractive index $n$ and impedance $z$ by [7,9,10]:

$$S_{11} = \frac{R_{01}(1 - e^{i2nk_0 d})}{1 - R_{01}^2 e^{i2nk_0 d}}, \tag{1a}$$

$$S_{21} = \frac{(1 - R_{01}^2)e^{ink_0 d}}{1 - R_{01}^2 e^{i2nk_0 d}}, \tag{1b}$$

where $R_{01} = z - 1/z + 1$.

As it has been pointed out in [4,5], the refractive index $n$ and the impedance $z$ are obtained by inverting Eqs. (1a) and (1b), yielding

$$z = \pm \sqrt{\frac{(1 + S_{11})^2 - S_{21}^2}{(1 - S_{11})^2 - S_{21}^2}}, \tag{2a}$$

$$e^{ink_0 d} = X \pm i\sqrt{1 - X^2}, \tag{2b}$$

where $X = 1/2S_{21}(1 - S_{11}^2 + S_{21}^2)$. Since the metamaterial under consideration is a passive medium, the signs in Eqs. (2a) and (2b) are determined by the requirement

$$z' \geqslant 0, \tag{3a}$$

$$n'' \geqslant 0, \tag{3b}$$

where $(\cdot)'$ and $(\cdot)''$ denote the real part and imaginary part operators, respectively. The value of refractive index $n$ can be determined from Eq. (2b) as

$$n = \frac{1}{k_0 d}\{[[\ln(e^{ink_0 d})]'' + 2\mathrm{m}\pi] - i[\ln(e^{ink_0 d})]'\}, \tag{4}$$

where m is an integer related to the branch index of $n'$. As mentioned above, the imaginary part of $n$ is uniquely determined, but the real part is complicated by the branches of the logarithm function.

Equations (2a) and (2b) can be directly applied in the case of a homogeneous slab for which the boundaries of the slab are well defined and the *S* parameters are accurately known. However, since a metamaterial itself is not homogeneous, the two apparently straightforward issues mentioned above need to be carefully addressed. First, the location of the two

 

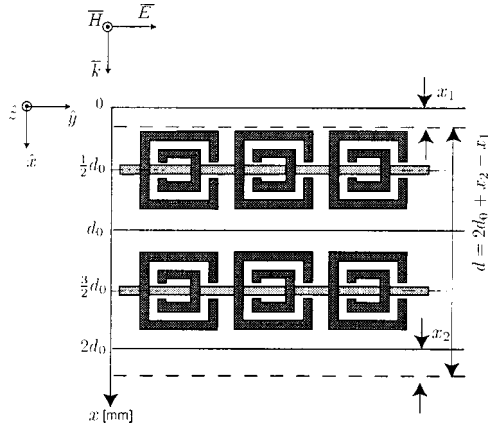


FIG. 1. Illustration of the effective boundaries of a two-cell metamaterial. The SRRs and rods are periodic along $\hat{y}$ and $\hat{z}$ directions with periodicity $a_y=4$ mm, $a_z=3$ mm. The unit-cell thickness ($d_0$) in the direction of wave incidence is 4 mm. We choose the first and the last unit-cell boundary as the reference plane for the parameters $x_1$ and $x_2$, respectively. The value of $x_1$ and $x_2$ are positive (negative) if the dashed lines are below (above) their reference planes. The thickness of the effective homogeneous medium is $2d_0+x_2-x_1$(mm).

boundaries of the effective slab need to be determined, which we do here by ensuring a constant impedance for various slab thicknesses. Second, the $S$ parameters obtained from numerical computation or measurements are noisy which can cause the retrieval method to fail, especially at those frequencies where $z$ and $n$ are sensitive to small variations of $S_{11}$ and $S_{21}$. These two problems are examined in detail in the following sections.

### B. Determination of the first boundary and the thickness of the effective slab

A homogeneous slab of material can be characterized by the fact that its impedance does not depend on its thickness. Our understanding of the physical meaning of the first effective boundary is a plane beyond which the reflected wave behaves like a plane wave for a plane wave incidence. When a plane wave is incident on a metamaterial, currents will be induced on the metals creating a scattered field. The field produced by the induced currents is not uniform: It is strongest around the metal and decay at a certain distance. The first effective boundary is located where the reflected wave behaves like a plane wave, and it has to be determined. We use $z_1$ and $z_2$ to represent the impedances of two slabs of metamaterial of different thicknesses. The reflection $S_{11}$ depends on the position of the first boundary and the transmission $S_{21}$ depends on the thickness of the slab. In addition, since the impedance $z$ is also a function of $S_{11}$ and $S_{21}$, $z$ depends on the first boundary and the thickness of the slab as well. Taking into account the above-mentioned properties, we propose a method whereby the first boundary and the thickness of the sample are determined by optimization so that $z_1$ matches $z_2$ at all frequencies. Figure 1 illustrates the configuration of the problem for a metamaterial made of two cells in the propagation direction ($x$ direction). The geometry of the metamaterial has been taken from [11,12], in which the dimensions have been slightly modified for ease of discretization in finite-difference time-domain (FDTD) simulations. With the split-ring resonator (SRR) and rod in the center of the unit cell, the periodicity along the propagation direction is $d_0$. The first boundary of the effective homogeneous medium is located at $x_1$ below ($x_1 \geqslant 0$) or above ($x_1 < 0$) the first unit-cell boundary, and the thickness of the effective medium is $2d_0+x_2-x_1$. The optimization model is set up to minimize the mismatch of impedances of different numbers of cells of metamaterial:

$$\min f(\overline{x}) = \frac{1}{N_f}\sum_{i=1}^{N_f} \frac{|z_1(f_i,\overline{x}) - z_2(f_i,\overline{x})|}{\max\{|z_1(f_i,\overline{x})|,|z_2(f_i,\overline{x})|\}},$$

$$\text{s.t.}: -0.5d_0 \leqslant x_1, \quad x_2 \leqslant 0.5d_0, \quad \overline{x} = (x_1,x_2), \tag{5}$$

where $N_f$ is the total number of sample frequencies and $z_j(f_i)$ represents the impedance of slab $j(j=1,2)$ at frequency $f_i$.

In the ideal case, $z_1$ matches $z_2$ for all frequencies with the objective function value equal to zero. We use the differential evolution algorithm [13] to optimize the objective function, and the optimized solution is $\overline{x_{\text{opt}}} = (3.8565\times10^{-4}d_0, 1.0479\times10^{-4}d_0)$. The corresponding values of impedance are shown in Fig. 2. It can be seen that the retrieved impedances for one, two, and three cells of SRR-rod metamaterial match well for most frequencies, while matching was not as satisfactory when the method in Ref. [4] was used (which corresponds to $x_1=0.5d_0$ in our formulation). We also calculated the impedance $z$ for the case of $\overline{x}=(0,0)$ and found that the results are almost the same as the optimized ones. We have corroborated this result with many other metamaterial thicknesses and geometries to eventually conclude empirically that the first effective boundary of a symmetric one-dimensional (1D) metamaterial [1,4,14] coincides with the first unit-cell boundary and the second effective boundary coincides with the last unit-cell boundary. For two-

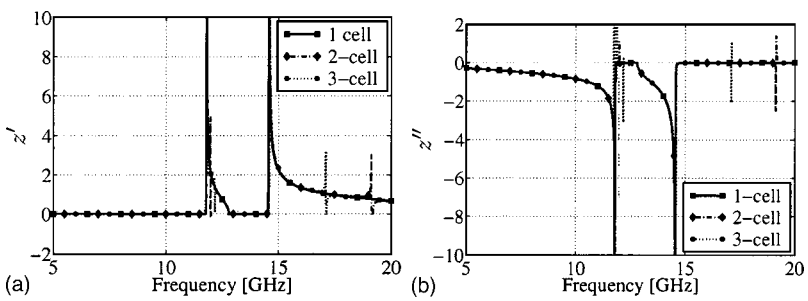


FIG. 2. Optimized impedance $z$ for one, two, and three cells of SRR-rod metamaterial of Fig. 1 in the direction of propagation.

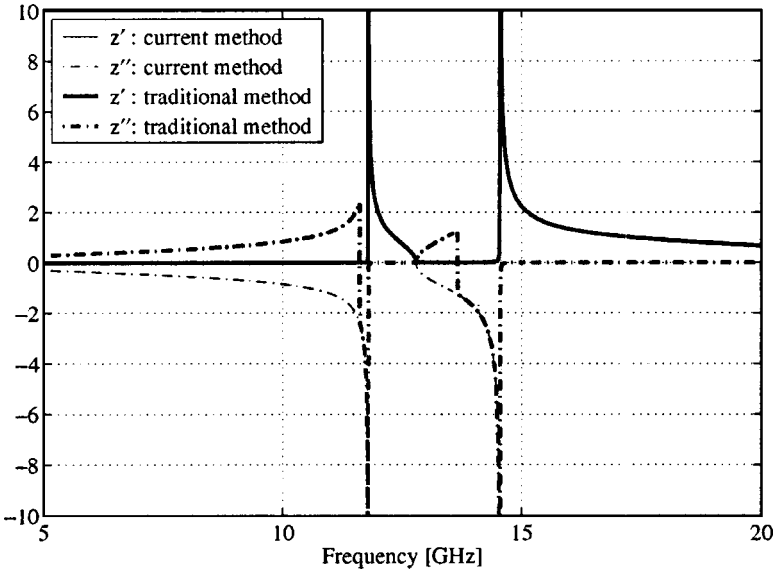


FIG. 3. Comparison of the retrieved impedance $z$ (real and imaginary parts) for one cell of metamaterial shown in Fig. 1 by the method presented in this paper and a traditional method using only the requirement $z' \geqslant 0$.

dimensional (2D) [11,14] and asymmetric 1D metamaterials, no such rule could be found and the effective boundaries of the slab need to be determined from optimization.

### C. Determination of $n$ and $z$ from $S_{11}$ and $S_{21}$

It is a common method to determine $z$ and $n$ from Eqs. (2a) and (2b) with the requirement of Eqs. (3a) and (3b), where $z$ and $n$ are determined independently. However this method may fail in practice when $z'$ and $n''$ are close to zero: A little perturbation of $S_{11}$ and $S_{21}$, easily produced in experimental measurements or numerical simulations, may change the sign of $z'$ and $n''$, making it unreliable to apply the requirement of Eqs. (3a) and (3b), as discussed in Ref. [6]. In fact, $z$ and $n$ are related and we should use their relationship to determine the signs in Eqs. (2a) and (2b). In order to determine the correct sign of $z$, we distinguish two cases. The first is for $|z'| \geqslant \delta_z$, where $\delta_z$ is a positive number, for which we apply Eq. (3a). In the second case, for $|z'| < \delta_z$, the sign of $z$ is determined so that the corresponding refractive index $n$ has a non-negative imaginary part, or equivalently $|e^{ink_0d}| \leqslant 1$, where $n$ is derived from Eqs. (1a) and (1b):

$$e^{ink_0d} = \frac{S_{21}}{1 - S_{11}\dfrac{z-1}{z+1}}. \tag{6}$$

Note that once we obtain the value of $z$, the value of $e^{ink_0d}$ is obtained from Eq. (6), so that we avoid the sign ambiguity in Eq. (2b) [it can be proven that only one sign of the imaginary part in Eq. (2b) makes it equivalent to Eq. (6)]. Figure 3 shows the retrieved impedance using the method presented in this paper and using only the condition of Eq. (3a). It is noted that the discontinuities obtained when only applying the criterion $z' \geqslant 0$ are removed.

### D. Determination of the branch of $n'$

We have presented in the previous sections a method of solving for $z$ and $n''$, but $n'$ remains ambiguous because of the branches of logarithm function as seen in Eq. (4). In order to address this problem, it has been suggested to use a slab of small thickness and applying the requirement that $\epsilon(f)$ and $\mu(f)$ are continuous functions of frequency [4,5]. However, no further details on the continuity argument were provided. In our method, we determine the proper branch by using the mathematical continuity of the parameters, with special attention to possible discontinuities due to resonances. The method is an iterative one: Assuming we have obtained the value of the refractive index $n(f_0)$ at frequency $f_0$, we obtain $n(f_1)$ at the next frequency sample $f_1$ by expanding the function $e^{in(f_1)k_0(f_1)d}$ in a Taylor series:

$$e^{in(f_1)k_0(f_1)d} \approx e^{in(f_0)k_0(f_0)d}\left(1 + \Delta + \frac{1}{2}\Delta^2\right), \tag{7}$$

where $\Delta = in(f_1)k_0(f_1)d - in(f_0)k_0(f_0)d$ and $k_0(f_0)$ denotes the wave number in free space at frequency $f_0$.

In Eq. (7), the branch index [m in Eq. (4)] of the real part of $n(f_1)$ is the only unknown. Since the left-hand side of Eq. (7) is obtained from Eq. (6), Eq. (7) is a binomial function of the unknown $n(f_1)$. Out of the two roots, one of them is an approximation of the true solution. Since we have obtained $n''(f_1)$, we choose the correct root among the two by comparing their imaginary parts with $n''(f_1)$. The root whose imaginary part is closest to $n''(f_1)$ is the correct one, and we denote it as $n_0$. Since $n_0$ is a good approximation of $n(f_1)$, we choose the integer m in Eq. (4) so that $n'(f_1)$ is as close to $n_0'$ as possible.

The branch of $n'$ at the initial frequency is determined as follows: From $\mu = nz$ and $\epsilon = n/z$, we have

$$\mu'' = n'z'' + n''z', \tag{8a}$$

$$\epsilon'' = \frac{1}{|z|^2}(-n'z'' + n''z'). \tag{8b}$$

The requirements $\mu'' \geqslant 0$ and $\epsilon'' \geqslant 0$ lead to

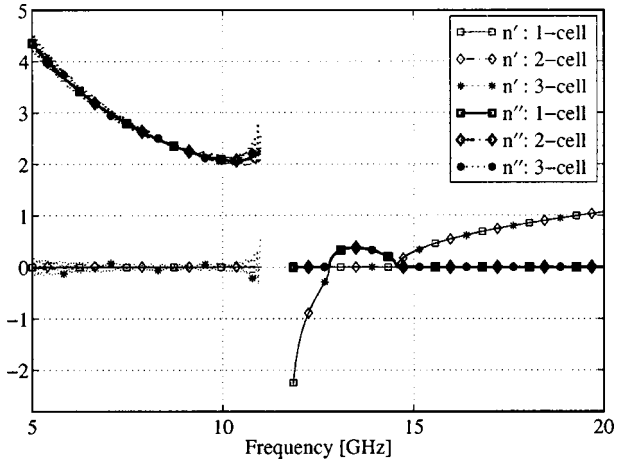


FIG. 4. Retrieved refractive index $n$ (real and imaginary parts) for one, two, and three cells of the metamaterial structure shown in Fig. 1.

$$|n'z''| \leqslant n''z'. \tag{9}$$

In particular, when $n''z'$ is close to zero but $z''$ is not, $n'$ should be close to zero. At the initial frequency, we solve for the branch integer $\mathsf{m}$ satisfying Eq. (9). If there is only one solution, it is the correct branch. In case of multiple solutions, for each of the candidate branch index $\mathsf{m}$, we determine the value of $n'$ at all subsequent frequencies using the above-mentioned iterative method. Because the requirement of Eq. (9) applies to $n'$ at all frequencies, we use it to check the validity of $n'$ at all frequencies produced by the candidate initial branch. Note in the special case when $n''z'$ is close to zero but $z''$ is not, the checking process can easily be carried out. Therefore, the initial branch that satisfies Eq. (9) at both the initial frequency and the subsequent frequencies is the correct one.

For the SRR-rod structure, we found that there is a frequency region at which there is no branch index $\mathsf{m}$ satisfying Eq. (9). We call this frequency region the resonance band. The properties of the resonance band are still disputed by researchers. Some papers [15–17] mention the existence of multiple modes in this region since the real part of $n$ is large, yielding a wavelength comparable to or smaller than the unit size of the metamaterial thereby rendering the retrieval of the effective parameters of the metamaterials impossible. Other papers [5,18] state that retrieval is possible and the retrieved permittivity $\epsilon$ has a negative imaginary part in the resonance band. In this paper, we do not address this issue and for this reason the retrieved results presented here are interrupted in frequency by the resonance region (see, for example, Fig. 4). In this case, since $n(f)$ is not continuous through all frequencies, we have to determine the initial branches for two frequency regions: Below and above the resonance band. Note that below the resonant band, the retrieved branch index is zero, which confirms the validity of the traditional method used for low-frequency retrieval. The retrieved refractive indexes $n$ for one, two, and three cells in the propagation direction are shown in Fig. 4, where the resonance band is seen to extend between 11 GHz and 12 GHz. We observe that the values of $n$ for different cell numbers are identical above the resonant region. Below the resonant band, however, the retrieved $n$ for one and two cells match well, but the result for three cells differs significantly from the previous two. This discrepancy is due to the small magnitude of $S_{21}$ in this frequency band, as we shall discuss in the next section.

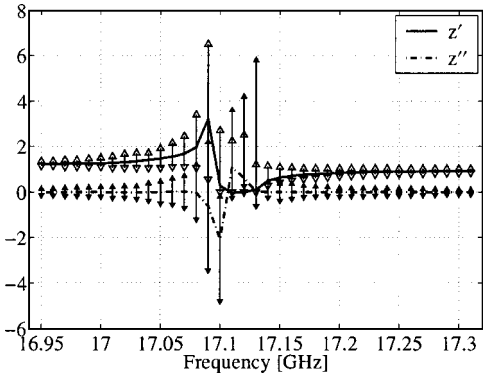


FIG. 5. Range of $z$ (real and imaginary parts) for tolerance $\delta_r = 0.015$ and $\delta_t = 0.0$ in Eqs. (11a) and (11b). The impedance is for a three-cell metamaterial shown in Fig. 1.

### E. Sensitivity analysis

A close examination of the retrieved $z$ and $n$ for one, two, and three cells of metamaterial presented so far shows that the three results do not always match. There are two cases of discrepancies. The first is that the retrieved refractive index $n$ for three cells of metamaterial does not match the value for one and two cells at low frequencies (5 GHz–11 GHz in Fig. 4). The second is that the impedance $z$ appears to spike at some frequencies (around 12 GHz, 17 GHz, and 19.5 GHz in Fig. 2). We shall show here that these discrepancies are due to the sensitivity of $z$ and $n$ to the accuracy of $S_{11}$ and $S_{21}$.

The first case appears when $|S_{21}|$ is close to zero. In the region below the resonance band, the transmission is usually small, especially for thicker metamaterials. From Eq. (2b), we see that $S_{21}$ appears in the denominator, so that the values of $n$ are very sensitive to small perturbations of $S_{21}$. Yet, a small transmission has little influence on the retrieval of $z$, which can be seen by computing:

$$\frac{\partial z^2}{\partial S_{21}} = \frac{8S_{21}S_{11}}{[(1-S_{11})^2 - S_{21}^2]^2}, \tag{10}$$

from which it is clear that a small $|S_{21}|$ makes $\partial z^2/\partial S_{21}$ small (approximately zero). In addition, we can see from Eq. (1b) that if $n''$ is not small, $S_{21}$ will decrease exponentially with $d$, i.e., with an increasing number of cells in the propagation direction. Therefore, the smaller $S_{21}$, the higher the computation and measurement relative errors, which leads to less accurate retrieval results.

The second case appears when $S_{21}^2$ is close to unity while $S_{11}$ is close to zero. Similar to the first case, the denominator in the expression of $z$ [see Eq. (2a)] approaches zero, thus making it difficult to retrieve $z$. However, in this case, the value of $n$ is stable. In this situation, instead of solving for $n$

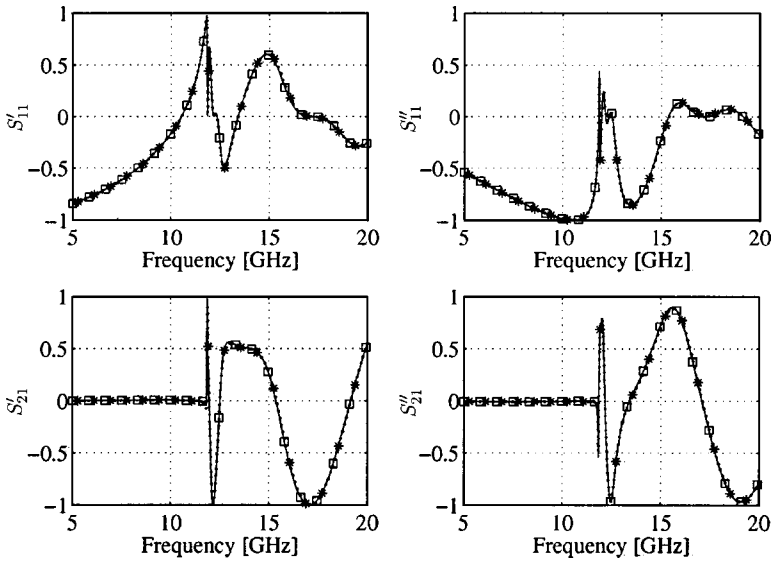


FIG. 6. $S_{11}$ and $S_{21}$ (real and imaginary parts) for three cells: Comparison between FDTD results (dot line with *) and calculated $S$ parameters based on the retrieved $\epsilon$ and $\mu$ (solid line with □) for a one-cell metamaterial shown in Fig. 1.

and $z$ which exactly satisfy Eqs. (1a) and (1b), we solve for the following inequalities:

$$\left| S_{11} - \frac{R_{01}(1 - e^{i2nk_0d})}{1 - R_{01}^2 e^{i2nk_0d}} \right| \leqslant \delta_r, \tag{11a}$$

$$\left| S_{21} - \frac{(1 - R_{01}^2)e^{ink_0d}}{1 - R_{01}^2 e^{i2nk_0d}} \right| \leqslant \delta_t, \tag{11b}$$

where $\delta_r$ and $\delta_t$ are small positive numbers. Figure 5 shows the range of $z$ satisfying Eqs. (11a) and (11b) for $\delta_r = 0.015$ and $\delta_t = 0.0$. At each frequency, all $z$ having a real and imaginary parts between the bounds shown in Fig. 5 satisfy Eqs. (11a) and (11b). It can be seen that the magnitude of the spikes is within the tolerance error, which implies that they are due to the noise in the $S_{11}$ and $S_{21}$ data.

Finally, note that although the retrieved $n$ and $z$ for multiple cells may be different from that for one cell at some specific frequencies, the calculated $S_{11}$ and $S_{21}$ for multiple cells using the retrieved $\epsilon$ and $\mu$ from one cell data match well with the $S_{11}$ and $S_{21}$ data computed for multiple cells directly from numerical simulation, as is illustrated in Fig. 6.

### F. Results

The retrieved permittivity $\epsilon$ and permeability $\mu$ of a one cell of SRR-rod structure of Fig. 1 are shown in Fig. 7. Note that although the results satisfy the condition $\epsilon'' \geqslant 0$ and $\mu'' \geqslant 0$, the positive energy requirement $\partial(\epsilon\omega)/\partial\omega > 0$ [19,20] is violated in the frequency band 12 GHz–12.2 GHz. As a result, the resonance band is extended to 11 GHz–12.2 GHz, as shown by the vertical dashed lines in Fig. 7(a). The value of $\epsilon$ and $\mu$ are both negative in the frequency range 12.2 GHz–12.8 GHz, showing that in this band, the metamaterial exhibits a LH behavior. We also retrieved the effective parameters of four and five cells of metamaterial shown in Fig. 1, and the retrieval results are close to those for one, two, and three cells.

In addition, we also applied our method to retrieve the effective parameters of the structure taken from [14,21], as shown in the inset of Fig. 8(a). For a 1D structure, by matching the impedance $z$ for one and two cells of the metamaterial using the previously described method, we obtain $\overline{x}_{\text{opt}} = (2.2053 \times 10^{-3} d_0, 1.1356 \times 10^{-3} d_0)$, where $d_0$ is the length of unit cell. Again, we find that the two boundaries of the effective homogeneous medium are close to the outer unit-cell boundaries of the 1D metamaterial. Figure 8 shows the retrieved $z$, $n$, $\epsilon$, and $\mu$ for one cell of this metamaterial. It can be seen that the frequency range of 13.8 GHz–14.5 GHz is a LH band, which agrees with the conclusion in Ref. [14]. It should be noted, however, that for a 2D version of this metamaterial, the effective boundaries should be obtained from the optimization process, as they do not necessarily

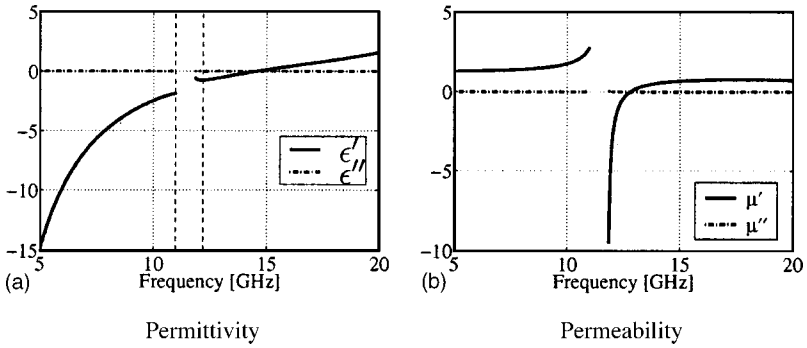


FIG. 7. Retrieved $\epsilon$ and $\mu$ (real and imaginary parts) for a one-cell metamaterial shown in Fig. 1. The vertical dashed lines denote the limits of the resonance band.

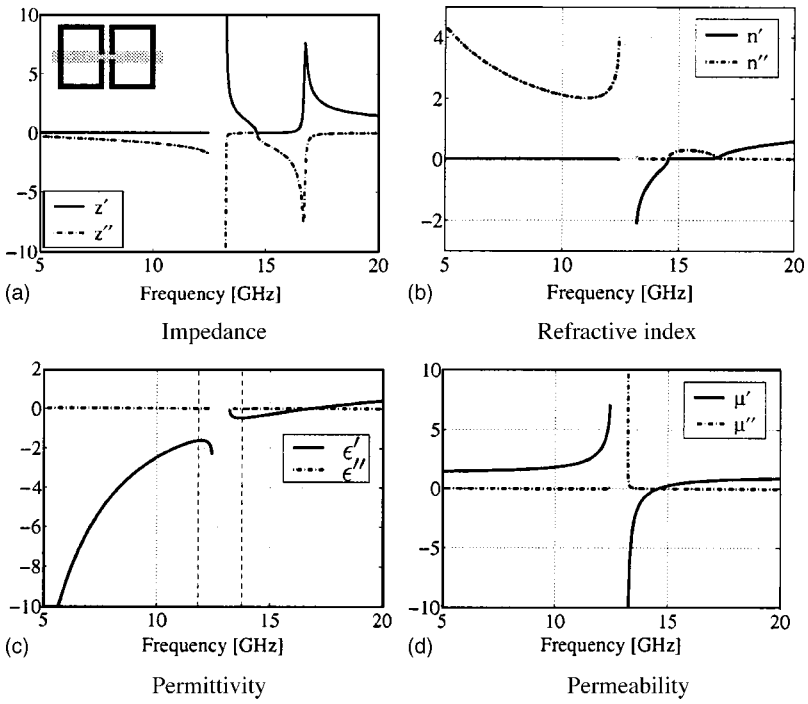


FIG. 8. Retrieved $z$, $n$, $\epsilon$, and $\mu$ (real and imaginary parts) for a one-cell metamaterial structure taken from Refs. [14,21] and shown in the inset (a). The vertical dashed lines denote the limits of the resonance band.

match the unit-cell boundaries of the metamaterial. Indeed, in this specific case, we obtain $\overline{x_{\text{opt}}}=(0.33110d_0, 0.30342d_0)$.

## III. CONCLUSION

We have proposed an improved method to retrieve the effective parameters (index of refraction, impedance, permittivity, and permeability) of metamaterials from transmission and reflection data. The successful retrieval results for various metamaterial structures show the effectiveness of the method. Our main conclusions are as follows:

(1) The first boundary and the thickness of the effective media can be determined by matching $z$ through all sample frequencies for different lengths of the slabs in the propagation direction. For symmetric 1D metamaterials, we have drawn the empirical conclusion that the first boundary coincides with the first boundary of the unit cell facing the incident wave, and the thickness of the effective medium is approximately equal to the number of unit cells multiplied by the length of a unit cell. For 2D and asymmetric 1D metamaterials, the effective boundaries have to be determined by optimization.

(2) The requirement $z' \geqslant 0$ cannot be used directly for practical retrievals when $z'$ is close to zero because the numerical or measurement errors may flip the sign of $z'$, making the result unreliable. In this case, we have to determine the sign of $z$ by the value of its corresponding $n$ so that $n'' \geqslant 0$.

(3) There is a resonance band characterized by the fact that the requirement $\mu'' \geqslant 0$ and $\epsilon'' \geqslant 0$ cannot be satisfied at those frequencies. On each side of the resonance, the branch of $n'$ can be obtained by a Taylor expansion approach considering the fact that the refractive index $n$ is a continuous function of frequency. Since the refractive index $n$ at the initial frequency determines the values of $n'$ at the subsequent frequencies, we determine the branch of the real part of $n$ at the initial frequency by requiring that $\mu''$ and $\epsilon''$ are non-negative across all the frequency band.

(4) Due to the noise contained in the $S$ parameters, the retrieved $n$ and $z$ at some specific frequencies are not reliable, especially for thicker metamaterials at lower frequencies. In spite of this, the fact that $S_{11}$ and $S_{21}$ for multiple cells of metamaterial calculated from the retrieved $\epsilon$ and $\mu$ for a unit-cell metamaterial match the $S_{11}$ and $S_{21}$ computed directly from numerical simulation confirms that the metamaterials can be treated as an effective homogeneous material.

## ACKNOWLEDGMENTS

This work was supported by DARPA (Contract No. N00014-03-1-0716) and ONR (Contact No. N00014-01-1-0713).

[1] D. R. Smith, W. J. Padilla, D. C. Vier, S. C. Nemat-Nasser, and S. Schultz, Phys. Rev. Lett. **84**, 4184 (2000).
[2] R. A. Shelby, D. R. Smith, and S. Schultz, Science **292**, 77 (2001).
[3] L. Ran, X. Zhang, K. Chen, T. M. Grzegorczyk, and J. A. Kong, Chin. Sci. Bull. **48**, 1325 (2003).
[4] D. R. Smith, S. Schultz, P. Markoš, and C. M. Soukoulis, Phys. Rev. B **65**, 195104 (2002).
[5] P. Markoš and C. M. Soukoulis, Opt. Express **11**, 649 (2003).
[6] R. W. Ziolkowshi, IEEE Trans. Antennas Propag. **51**, 1516

(2003).
[7] A. M. Nicolson and G. F. Ross, IEEE Trans. Instrum. Meas. **19**, 377 (1970).
[8] J. Baker-Jarvis, E. J. Vanzura, and W. Kissick, IEEE Trans. Microwave Theory Tech. **38**, 1096 (1990).
[9] J. A. Kong, *Electromagnetic Wave Theory* (EMW, Cambridge, MA, 2000).
[10] J. A. Kong, Prog. Electromagn. Res. **35**, 1 (2002).
[11] D. A. Shelby, D. R. Smith, S. C. Nemat-Nasser, and S. Schultz, Appl. Phys. Lett. **78**, 489 (2001).
[12] C. D. Moss, T. M. Grzegorczyk, Y. Zhang, and J. A. Kong, Prog. Electromagn. Res. **35**, 315 (2002).
[13] R. Storn and K. Price, J. Global Optim. **11**, 341 (1997).
[14] T. M. Grzegorczyk, C. D. Moss, J. Lu, and J. A. Kong, *New Ring Resonator for the Design of Left-Handed Materials at Microwave Frequencies*, Proceedings of Progress in Electromagnetics Research Symposium, Honolulu, Hawaii, 2003 (EMW, Cambridge, MA, 2003), p. 286.
[15] C. R. Simovski, P. A. Belov, and S. He, IEEE Trans. Antennas Propag. **51**, 2582 (2003).
[16] J. E. Sipe and J. V. Lranendonk, Phys. Rev. A **9**, 1806 (1974).
[17] P. A. Belov, S. A. Tretyakov, and A. J. Viitanen, Phys. Rev. E **66**, 016608 (2002).
[18] T. Koschny, P. Markoš, D. R. Smith, and C. M. Soukoulis, Phys. Rev. E **68**, 065602 (2003).
[19] L. D. Landau, E. M. Lifshitz, and L. P. Pitaevskii, *Electrodynamics of Continuous Media*, 2nd ed. (Pergamon, Oxford, 1984).
[20] V. Veselago, Sov. Phys. Usp. **10**, 509 (1968).
[21] C. D. Moss, Ph.D. thesis, Massachusetts Institute of Technology, 2004.